NeuroImage 224 (2021) 117403

Contents lists available at ScienceDirect

NeuroImage

journal homepage: www.elsevier.com/locate/neuroimage

Neural correlates of future weight loss reveal a possible role for brain-gastric interactions

Gidon Levakov[a,b,*], Alon Kaplan[c], Anat Yaskolka Meir[c], Ehud Rinott[c], Gal Tsaban[c], Hila Zelicha[c], Nachshon Meiran[b,d], Ilan Shelef[b,e], Iris Shai[c], Galia Avidan[a,b,d]

[a] Department of Brain and Cognitive Sciences, Ben-Gurion University of the Negev, Beer-Sheva, Israel
[b] Zlotowski Center for Neuroscience, Ben-Gurion University of the Negev, Beer-Sheva, Israel
[c] Department of Epidemiology, Ben-Gurion University of the Negev, Beer-Sheva, Israel
[d] Department of Psychology, Ben-Gurion University of the Negev, Beer-Sheva, Israel
[e] Department of Diagnostic Imaging, Ben-Gurion University of the Negev, Beer-Sheva, Israel

ARTICLE INFO

Keywords:
Lifestyle intervention
Functional connectivity
Obesity
Gastric network
Stomach
Mediterranean diet
Physical activity

ABSTRACT

Lifestyle dietary interventions are an essential practice in treating obesity, hence neural factors that may assist in predicting individual treatment success are of great significance. Here, in a prospective, open-label, three arms study, we examined the correlation between brain resting-state functional connectivity measured at baseline and weight loss following 6 months of lifestyle intervention in 92 overweight participants. We report a robust subnetwork composed mainly of sensory and motor cortical regions, whose edges correlated with future weight loss. This effect was found regardless of intervention group. Importantly, this main finding was further corroborated using a stringent connectivity-based prediction model assessed with cross-validation thus attesting to its robustness. The engagement of senso-motor regions in this subnetwork is consistent with the over-sensitivity to food cues theory of weight regulation. Finally, we tested an additional hypothesis regarding the role of brain-gastric interaction in this subnetwork, considering recent findings of a cortical network synchronized with gastric activity. Accordingly, we found a significant spatial overlap with the subnetwork reported in the present study. Moreover, power in the gastric basal electric frequency within our reported subnetwork negatively correlated with future weight loss. This finding was specific to the weight loss related subnetwork and to the gastric basal frequency. These findings should be further corroborated by combining direct recordings of gastric activity in future studies. Taken together, these intriguing results may have important implications for our understanding of the etiology of obesity and the mechanism of response to dietary intervention.

1. Introduction

Over the last decades, obesity rates increased drastically, while evidence for its negative impact on health has been accumulated (Mokdad et al., 1999; Wang et al., 2008). The complex etiology includes metabolism, cognition, eating behaviors and gut-microbiome (Proctor et al., 2017). Assessing whether and how such different aspects can predict treatment success is an ongoing effort (MacLean et al., 2018). Accordingly, there has been a growing interest in the neural and cognitive factors that may be associated with successful weight regulation. In the current work, we attempted to characterize functional neural correlates of future weight loss. We further interpret these results and examine whether they support one of the existing prominent neural theories of weight regulation. A recently published review presented such three potential neural factors associated with impaired weight regulation (Stice and Yokum, 2016) including: 1. Over-sensitivity to palatable food cues; 2. A deficit in inhibitory control and 3. Abnormal reward processing. Our neural findings provide support for the over-sensitivity to food cues theory and do not obviously relate to the other two factors listed above. We therefore propose a possible novel account linking brain–gut interactions to functional brain connectivity and weight loss, although the gastric activity was not recorded in the current work. Below we lay out the relevant background on resting-state functional connectivity, brain–gut interactions and weight regulation.

1.1. Neural attributes related to future weight loss

The three above-mentioned theories of impaired weight regulation gain support from recent prospective, longitudinal and randomized interventional imaging studies. While some studies examined brain ac-

* Corresponding author at: Department of Brain and Cognitive Sciences, Ben-Gurion University of the Negev, Beer-Sheva, Israel
E-mail address: gidonle@post.bgu.ac.il (G. Levakov).

https://doi.org/10.1016/j.neuroimage.2020.117403
Received 17 February 2020; Received in revised form 19 August 2020; Accepted 25 August 2020
Available online 23 September 2020

tivation in response to specific stimuli or tasks, others characterized brain activity using resting-state functional connectivity (RSFC) analysis. This approach examines coactivation patterns between brain regions in order to assess network connectivity, rather than the signal in a specific region. Such brain connectivity patterns or 'connectome' (Sporns et al., 2005), even when measured at rest, exhibit a typical organization into communities or subnetworks (Bullmore and Sporns, 2009). Moreover, they are reliable across scan sessions and reflect individual differences in different domains such as perception and executive functions (Boly et al., 2007; Finn et al., 2015; Lerman-Sinkoff et al., 2017; Nomi et al., 2017). Of the three aforementioned theories, multiple findings converge best with the over-sensitivity theory (Stice and Burger, 2019). According to this theory, increased response to external sensory cues of food, learned by conditioning, results in overeating and impaired weight regulation ability. In line with this notion, visual and olfactory food cues elicited elevated brain activity in somatosensory, visual and gustatory cortices, and such signals were positively correlated with immediate energy consumption (Burger and Stice, 2013) and future weight gain (Stice and Yokum, 2018). Moreover, RSFC within the saliency network, previously suggested to underlie increased baseline susceptibility to food cues in obesity (García-García et al., 2013), was found to decrease following meal intake while the magnitude of this reduction correlated with body fat (Sewaybricker et al., 2019). Unlike the over-sensitivity theory, the reward theory relates difficulties in weight regulation to an innate increased neural reward response to food consumption. Accordingly, BOLD activation (Geha et al., 2013) and neural variability (Kroemer et al., 2016) in response to food intake predicted future weight loss in the striatum, typically involved in reward processing. Furthermore, RSFC in the striatum was found to correlate with food craving and predicted future weight gain (Contreras-Rodríguez et al., 2017). Lastly, the inhibitory control theory pertains impaired weight regulation to a deficit in executive function (Friedman and Miyake, 2017) and specifically, in inhibitory control. Deficits in inhibitory control are thought to impede attempts to avoid palatable food or resist previous eating habits when actively attempting to lose weight. Consistently with this account, studies reported that activation within the DLPFC during typical (Lavagnino et al., 2016) and food-related (Han et al., 2018) inhibitory control tasks was negativity correlated with body-mass index (BMI). Furthermore, regional connectivity within the DLPFC (Dong et al., 2015) and its connectivity to the ventromedial prefrontal cortex (Neseliler et al., 2019; Weygandt et al., 2013), positivity correlated with future weight loss. In light of the abundance of behavioral evidence supporting the significant role of executive function in modulating health-related choices and regulation of eating behavior (Gettens and Gorin, 2017), in the current study, executive function behavioral measures were assessed at baseline. These measurements are part of a separate line of work focusing on the correlation of executive function behavioral scores with future weight loss (Kaplan et al., 2019, Manuscript in preparation) and are used here only to shed light on the inhibitory control neural hypothesis.

1.2. Brain-gut communication and control of appetite

Hunger and satiety signals from the periphery to the brain have a major influence on eating behavior. They are evident in multiple routes, mainly direct vagal and spinal innervation and hormonal signaling originating from the gastrointestinal (GI) tract (Steinert et al., 2012). Within the GI tract, appetite-related signals originating from the stomach are considered the most immediate and salient (Cummings and Overduin, 2007; Park and Camilleri, 2005). They include an indication of the gastric nutritional content (de Araujo et al., 2008), as well as distention and emptying stage (Steinert et al., 2012). Gastric motility is achieved by slow-wave contractions that increase in amplitude during phase III of the migrating motor complex (MMC), a pattern of mechanical and electrical activity that features while fasting (Sarna, 1985). Phase III of the MMC, a short phase of maximal peristaltic activity, was found to be related to peaks in hunger sensation (Tack et al., 2016). These contractions are initiated and coordinated by electrical activity in the interstitial cells of Cajal (Sanders et al., 2006) and present a typical 0.05Hz frequency. Recent evidence implies that a network of cortical regions shows high synchrony with this gastric basal electrical activity as measured during resting state (Rebollo et al., 2018). In this recent study, subjects' gastric electrical activity was recorded using cutaneous electrodes, while conducting an fMRI resting-state session. The authors reported that a network of cortical regions, typically related to sensory and motor functions, showed delayed synchrony with this electrical activity. Importantly, this phase-locking between the stomach electrical activity and the BOLD signal was specific to the gastric basal 0.05 Hz frequency and a previous study (Richter et al., 2017) suggested that it arises from gastric, rather than cortical activity.

1.3. The present study

Our goal was to examine whether and how RSFC, as measured with fMRI may predict future weight loss in a lifestyle dietary intervention. We use of the term *prediction* here due to the temporal precedence of the predictive variable, resting-state connectivity, to the predicted variable, weight loss following intervention that began only after the brain imaging session. However, we would like to make it clear that 'prediction' does not imply causation in this context, since it is possible that the future weight loss is merely a reflection of a trait that was already present when the brain scan was taken. To the best of our knowledge, to date, only a single study attempted to characterize whole-brain RS connectivity patterns in relation to weight regulation, in contrast to connectivity of specific ROIs (Mokhtari et al., 2018). Specifically, in this study, RS connectivity and machine learning classification were used to evaluate weight loss in an 18-month lifestyle weight loss intervention. The authors described multiple subnetworks that are typically involved in cognitive control, body awareness, and food perception whose dynamic properties predicted future weight loss. However, in the current study, we employed a more straightforward methodology that allowed us to directly interpret the neural-cognitive predictors of future weight loss. Moreover, we recorded a substantially longer RS session (14 min) within a large sample size (n = 92). The current study is prospective, open-label with three arms and was conducted as part of a large-scale lifestyle intervention study (Yaskolka Meir et al., 2019). At baseline, prior to the intervention, both the brain imaging sessions and a battery of behavioral executive function tests were conducted. Executive function scores were used to examine whether RSFC correlates of weight loss are related to executive function abilities, in line with the inhibitory control hypothesis. Weight loss values were measured after a 6-month follow up, that is considered a crucial period where maximum weight loss is typically achieved (Shai et al., 2008). Network analysis was carried out by utilizing the Network-Based Statistic procedure (NBS; Zalesky et al., 2010), which is a common method for addressing the multiple comparisons problem in whole-brain connectivity analysis. Specifically, this method looks for sets of connected nodes or subnetworks whose edges differ across experimental groups or are correlated with specific measured variables (e.g. weight loss). Moreover, we utilized the Connectome-based Predictive Modeling scheme (CPM; Shen et al., 2017) to quantify the extent to which such subnetworks can accurately predict future weight loss using cross-validation. Finally, we propose a post-hoc hypothesis regarding the importance of brain-gastric interactions for successful weight loss. Although the gastric activity was not directly recorded in the current work, we provide evidence of a spatial and temporal similarity of the detected subnetwork to the gastric network reported by Rebollo et al. (2018).

2. Methods

2.1. Participants

Two hundred and ninety-four participants enrolled in the Dietary Intervention RandomizEd Controlled Trial PoLyphenols UnproceSsed

Table 1
Baseline characteristics of the functional connectivity sub-study by intervention group. The statistical data are presented for subjects who completed the executive function battery, weight measurements, fMRI resting-state session and were not excluded due to excessive motion (see Section 2.6.). Weight loss was reported as percent weight loss from baseline to time-point 6 (see Fig. 1 for details). Table cells present the mean (± standard deviation) or case counts. F = female, M = male, PA = Physical activity, MED = Mediterranean, BMI = body mass index, WC = waist circumference.

	PA	PA+MED	PA+MED+ polyphenols	All group
N	29	29	34	92
Weight (kg)	90.3 (± 12.5)	91.25 (± 10.5)	90.3 (± 10.0)	90.6 (± 10.9)
Gender	F: 4; M: 25	F: 4; M: 25	F: 3; M: 31	F: 11; M: 81
Height (cm)	172.7 (± 7.9)	175.6 (± 7.2)	173.8 (± 7.4)	174.0 (± 7.5)
BMI ($kg/m^{2)}$	30.2 (±3.3)	29.6 (± 3.1)	29.9 (± 3.0)	29.9 (± 3.1)
WC (cm)	107.6 (± 9.4)	107.6 (± 6.5)	106.9 (± 7.1)	107.3 (± 7.6)
Age (y)	49.3 (±10.6)	49.0 (±9.8)	49.3 (±10.9)	49.2 (±10.3)
Weight loss (%)	2.47 (± 4.0)	7.25 (± 5.8)	5.86 (± 5.8)	5.2 (± 5.6)

(DIRECT-PLUS), testing the influence of Mediterranean (MED), and polyphenol-enriched MED diet on participants' health. Subjects were all recruited from an isolated workplace with a monitored provided lunch (Nuclear Research Center Negev, Dimona, Israel). Reflecting the study's workplace profile, only 12% of participants were female. Inclusion criteria were based on large waist circumference (WC; men > 102 cm, women > 88 cm) or dyslipidemia (TG>150 mg/dl and HDL-c <40 mg/dL for men and <50 mg/dL for women) and age (>30). Exclusion criteria included individuals who were unable to adhere to a physical activity (PA) program due to medical reasons or serum creatinine ≥2 mg/dL, disturbed liver function, pregnancy, active cancer patients, those who underwent chemotherapy in the last 3 y, a major illness that might require hospitalization and those with a pacemaker or platinum implant, given the use of MRI. We note that usage of central acting medications was not considered an exclusion criterion but nevertheless, subjects were asked to report this information as part of the study. All participants provided informed consent and the study was approved by the Human Subject Committee of Soroka Medical Center. This trial was registered at clinicaltrials.gov as NCT03020186. Of the 294 subjects that started the intervention 212 completed an executive function battery (see Section 2.10) at baseline. The functional connectivity sub-study described in the present paper includes 132 subjects who completed both the executive function battery and two baseline rsfMRI scans acquired consecutively during the same session. Of these 132 subjects, 40 were excluded due to excessive motion (see Section 2.6). Hence, data from 92 subjects was used for all the functional connectivity analyses. Only 2.2% of these subjects reported using central acting medications (2 out of 92), thus excluding this factor as a potential confound that might affect functional connectivity measures. Table 1 provides the baseline characteristics of all 92 participants.

2.2. Study design

This sub-study is prospective, open-label with three arms, conducted as part of a large randomized controlled intervention trial that was initiated in May 2017 and lasted for 18 months. First, in a period of 5 months, baseline measurements that included brain imaging and behavioral executive function scores were taken for all participants. After baseline measurements, participants were assigned to one of three intervention groups: PA; PA + Mediterranean (MED) diet; PA + polyphenol-enriched MED diet and their initial weight was taken. Group assignment was done randomly within strata of age. Following 6 months of lifestyle intervention, which are considered a rapid weight loss phase, weight measurements were taken again and percent weight loss relative to baseline was computed for each subject as the main outcome of interest in the current study. See Fig. 1 for a graphical description of the study design and timeline.

2.3. Intervention

PA - All groups received free gym memberships and moderate-intensity, ~80% aerobic PA classes within their workplace. *PA + MED* – In addition to the PA component common to all groups, participants in this group were instructed to follow calorie-restricted traditional Mediterranean diet as described in previous work (DIRECT study; Shai et al., 2008). *PA + polyphenol-enriched MED diet* – participants in this group received a diet that was lower in processed and red meat than the MED diet and richer in plants and polyphenols. Polyphenols are large organic molecules typically found in fruits, vegetables, green tea, coffee and red wine (D'Archivio et al., 2010) and were previously suggested to have a positive effect on cardiovascular health (Pang et al., 2016). Further elaboration on the intervention procedure is provided in a separate study (Yaskolka Meir et al., 2019).

2.4. Weight loss

Weight was measured at baseline, and after 6 months of intervention, that is considered a rapid weight loss phase in which maximum weight loss is achieved (Shai et al., 2008). Following 6 months of intervention, the 92 participants of the brain functional connectivity sub-study lost 2.47% (± 4.0), 7.25% (± 5.8), and 5.86% (± 5.8) of their initial weight for the PA, PA+MED and polyphenol-enriched MED diet groups respectively. To assess participants' weight loss independently of the specific dietary intervention they received, weight loss is reported as the percent of the weight a participant decreased from their initial weight after controlling for the effect of the specific intervention group.

2.5. MRI scanning procedure

MRI scans were conducted at the Soroka University Medical Center (SUMC), Beer Sheva, Israel. Participants were scanned in a 3T Philips Ingenia scanner (Amsterdam, The Netherlands) equipped with a standard head coil. All subjects were instructed to refrain from food and non-water beverages two hours prior to the MRI sessions. Each session included 2 RS-fMRI runs of 7 min each, and a 3D T1-weighted anatomical scan to allow registration of the functional data. Before each RS session, subjects were instructed to remain awake with their eyes open and lie still. Both resting-state scans were acquired back-to-back with a few seconds apart during which the researchers communicated with the participants and reminded them to stay awake and lie still. fMRI BOLD contrast was acquired using the gradient-echo echo-planner imaging sequence with parallel acquisition (SENSE: factor 2.2). Specific scanning parameters were as follows: whole-brain coverage 41 slices ($3 \times 3 \times 3$ mm^3), transverse orientation, 3 mm thickness, no gap, TR = 2200 ms, TE = 30 ms, flip angle=90°, FOV = 200 × 222 (RL × AP) and matrix size 68 × 71 (RL × AP). High-resolution anatomical volumes

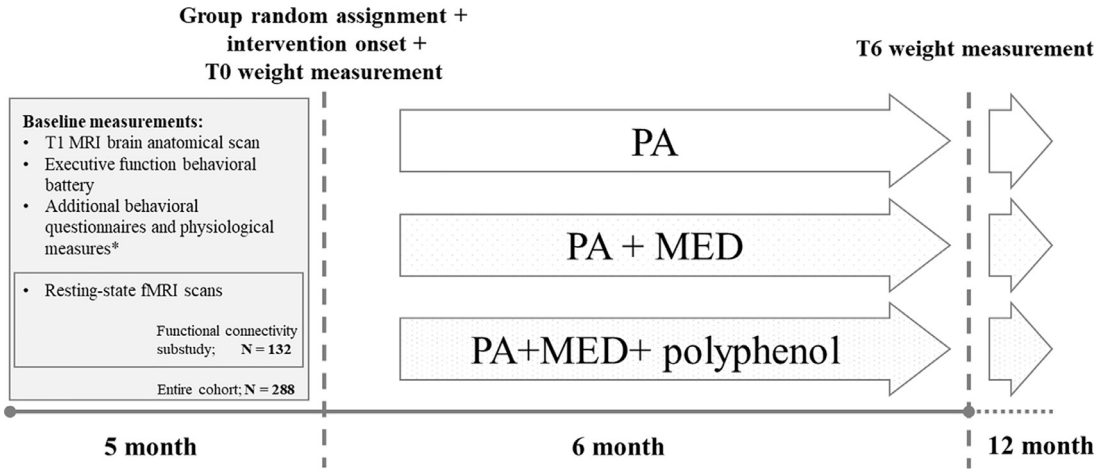

Fig. 1. Study design and timeline. For a period of 5 months, baseline measurements including brain imaging and behavioral executive function scores were taken for all subjects. Next, participants were assigned to one of three intervention groups: PA; PA + Mediterranean (MED) diet; PA + polyphenol-enriched MED diet and their initial weight was measured. Each group underwent eighteen months of lifestyle intervention, of which, the initial 6 months were considered the rapid weight loss phase (Shai et al., 2008). In time point 6, 6 months after intervention onset, weight measurements were taken again, and percent weight loss relative to the initial weight was computed for each subject as the main outcome of interest. T0 = intervention onset, T6 = 6 month after intervention onset. * = see Yaskolka Meir et al. (2019) for further elaboration on the baseline measurements.

were acquired with a T1-weighted 3D pulse sequence ($1 \times 1 \times 1$ mm^3, 150 slices).

2.6. fMRI data analysis

fMRI preprocessing was performed using the Configurable Pipeline for the Analysis of Connectomes (C-PAC; Cameron et al., 2013) and included: slice time correction, motion correction, skull stripping, nuisance regression of the first 5 principal components (PCs) of signal from white matter and CSF (Behzadi et al., 2007), 6 motion parameters and linear and quadratic trends, followed by temporal filtering between 0.1 and 0.01 Hz and global signal regression. Finally, a scrubbing threshold of 0.5 mm frame-wise displacement (Power et al., 2014; removal of 1 TR before and 2 TR after excessive movement) was applied. All the results were reproduced without the scrubbing procedure (see Supplementary Section 2). The resting-state sessions exhibit relatively high between-run reliability for both the scrubbed (cross-run correlation: $M = 0.699$, SD = 0.072; root-mean-square deviation: $M = 0.201$, SD = 0.023) and un-scrubbed data (cross-run correlation: $M = 0.715$, SD = 0.066; root-mean-square deviation: $M = 0.197$, SD = 0.021) that is also consistent with previous reports (Birn et al., 2013) and thus were concatenated for all following analysis. Exclusion criterion for excessive movements was determined a priori to less than 7 min (50%) of the resting-state session after the scrubbing procedure (30% omitted; 92 subjects left). For the purpose of structural brain delineation, anatomical scans were analyzed using FreeSurfer version 6 (Fischl et al., 1999, 2004). The integration of the different tools was done using Nipype (Gorgolewski et al., 2011).

2.7. Subnetwork definition

Vertices were defined using the Lausanne 128 nodes (114 cortical + 14 subcortical) parcellation (Hagmann et al., 2008) created with Connectome Mapper (Daducci et al., 2012). Importantly the results were also reproducible using a finer 462 node resolution (see Supplementary Section 3). For most subjects (> 95%), the field of view did not capture the entire cerebellum and brainstem and hence we did not include these regions of interest (ROIs) in the analyses for the entire group. Functional connectivity was defined using Pearson correlation coefficients between each pair of vertices following a Fisher r-to-z'-transformation. Subnetworks were defined based on the 7 networks cortical parcellation defined by Yeo et al. (2011, Fig. 2).

2.8. Network-based statistic (NBS)

To estimate whole-brain functional connectivity characteristics that can predict subsequent weight loss, we used the Network-Based Statistic procedure (NBS; Zalesky et al., 2010). NBS is a common method used to detect connected components or subnetworks whose edges' strength differ across experimental groups or are correlated with a measured variable (i.e. weight loss in the current study). NBS controls for family-wise error rate (FWER) by comparing the size of the largest connected component to a distribution yielded by a permutation procedure. Briefly, the strength of each edge was correlated with the weight loss measurement, followed by a Fisher r-to-z'-transformation. Then, a threshold was applied to the subsequent correlation matrix, and the size of the largest connected component was retained. A connected component is a subnetwork in which any pair of nodes are connected with a path composed of above-threshold edges. The same procedure was repeated 10,000 times with the weight loss values permutated. The p-value of the subnetwork indicated the percent of times that a random component was larger than the empirical component. The applied threshold is the only free parameter in this model, thus it is essential to make sure the results are robust to a wide range of this parameter (Zalesky et al., 2010). Accordingly, starting from a value of z'=0.27 (p=0.01), we tested the effect of an increase or decrease of this value (±0.02) and reported the range in which the detected subnetwork was found significant (p<0.05). Our NBS implementation is available online (https://github.com/GidLev/NBS-correlation), and it is based on the brain connectivity toolbox (BCT; Rubinov and Sporns, 2010) and the BCTPY (https://github.com/aestrivex/bctpy) code.

2.9. Connectome-based Predictive Modeling (CPM)

Using idiosyncratic sample-based prediction as opposed to group differences statistical hypothesis testing, we adopted the *Connectome-based Predictive Modeling* CPM protocol (Shen et al., 2017). Applying a Leave-One-Out cross-validation approach, within the train set we correlated each edge in the connectivity matrix with weight loss measurement for each subject. We then selected the edges whose correlation with weight loss passed a predetermined threshold. To validate the robustness of the results the procedure was reproduced for a wide range of thresholds ($0.25 < r < 0.35$). Next, the values of the selected edges were summed for each subject, resulting in a single scalar that was used to fit a lin-

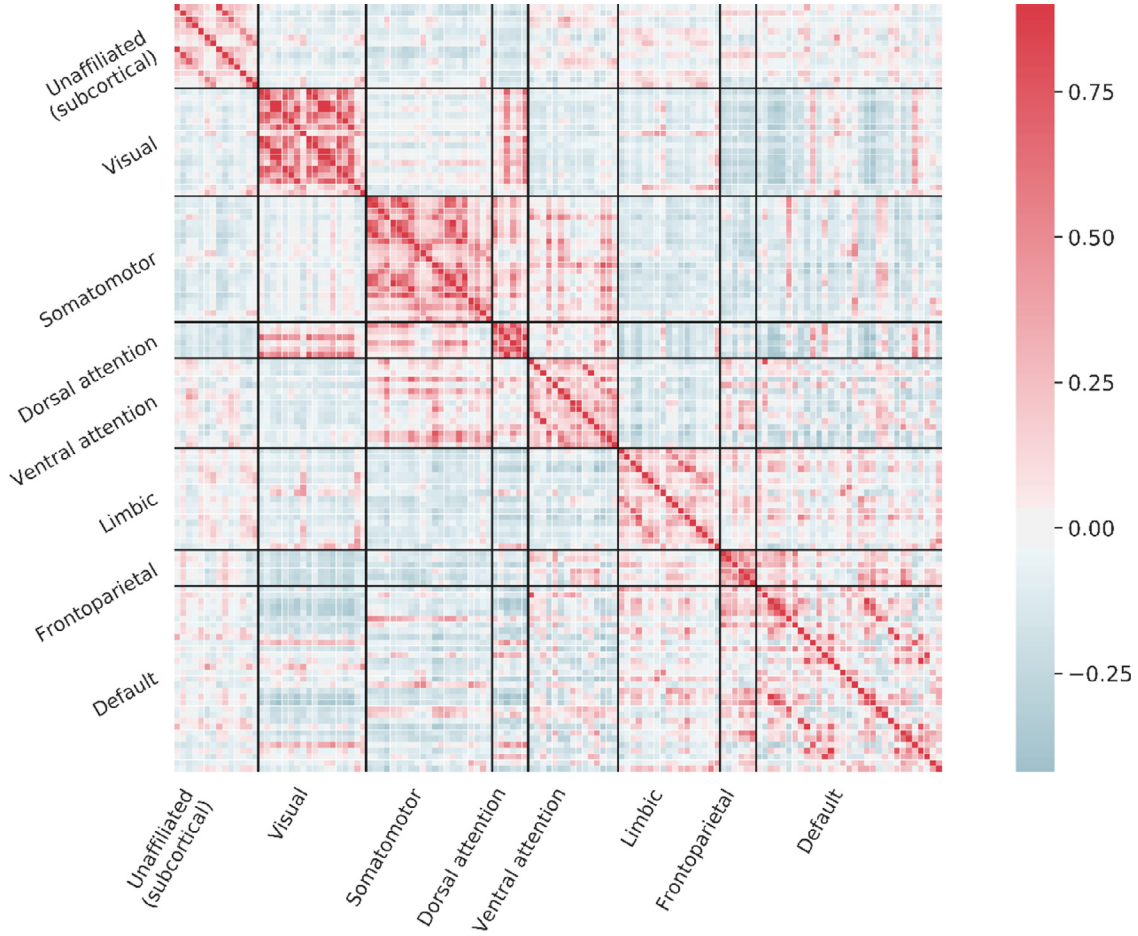

Fig. 2. Mean correlation matrix. The matrix represents all per-wise correlations among nodes' time series following Fisher *r*-to-*z*'-transformation, averaged across all participants. Nodes are grouped according to the Yeo-7 networks parcellation (separated by black lines; Yeo et al., 2011), such that the squares along the main diagonal represent within network connectivity. Networks order: unaffiliated (subcortical regions), visual, somatomotor, dorsal attention, ventral attention, limbic, frontoparietal, default. Nodes within each network are grouped by hemisphere.

ear model predicting weight loss within the training set. The model was then applied to the remaining test subject. It is crucial that edge selection and the linear regression model fitting is done only on the training set and then tested on the untouched, leave-one-out subject, as done here. Since the purpose of this study was to detect a connected component, rather than a sparse, unconnected set of edges, the summation of nodes was conducted only on edges that passed the threshold and formed the largest connected component, as in the NBS analysis (see Section 2.8).

2.10. Evaluation of executive function

Executive functions were measured using the Brief Executive Function Battery (BEF; Gordon et al., 2018) composed of the following measurements: Working memory was evaluated using accuracy differences between choice reaction time with 6 novel rules and a similar task with 2 practiced rules. Switching ability was quantified using accuracy differences between task-switching conditions (3 tasks, each involving two practiced rules) to the 2-practiced rules condition. Inhibition was assessed with the accuracy in the Anti-saccade task. General executive function was quantified as the 1st un-rotated PC of these three measurements. Subjects with an accuracy performance of less than 2 standard deviations from the mean in one of the tasks were excluded (14.1% omitted; 182 left). Executive function scores were analyzed, excluding when they were used as covariates for the RSFC measures, for all remaining subjects (n = 182). A more in-depth analysis of the measures of the executive function battery in relation to weight-loss is outside the scope of the present study (Kaplan et al., 2019, Manuscript in preparation).

2.11. Relation between weight loss, connectivity patterns and performance on executive function tasks

To compare behavioral executive function scores and RSFC as predictors of future weight loss, the explained variance of both was compared. Explained variance was computed as follows:

$$EV(y,\quad \hat{y}) = 1 - \frac{Var\{y-\hat{y}\}}{Var\{y\}}$$

EV = explained variance, y = true percent weight loss value, y hat = predicted percent weight loss value, *Var* = variance, i.e. the square root of the standard deviation.

Weight loss prediction with both measures was done using a univariate regression model with the 1st PC of the executive function scores and the sum of the suprathreshold edges in the CPM model. Importantly, for both weight loss predictors, explained variance was computed using a Leave-One-Out cross-validation. To examine the possible effect of executive function on RSFC, we employed an additional CPM model, in which prior to model fitting, the 1st PC of all three executive function scores was regressed out from each edge in the connectivity matrix.

2.12. Spatial comparison between the subnetwork detected in the present study to Rebollo et al. (2018) gastric network

To quantify the spatial similarity between the set of regions found using NBS in the current study and the set of significant regions in the gastric network reported in Rebollo et al. (2018; available online https://neurovault.org/images/51888/), we examined the percentage

Table 2
NBS results for different Pearson coefficient thresholds. In the NBS method, the strength of each edge is correlated with the weight loss values. Then, a threshold is applied to the subsequent correlation matrix, and the size of the largest connected component is retained. Each row in the table describes the applied threshold, the number of edges found in the largest connected component and the corresponding p-value indicating the percentage of times that a random component was larger than the empirical component. The weight loss related subnetwork was found significant across a wide range of thresholds ($z' = 0.25$, $0.29 \leq z' \leq 0.45$; all p's < 0.05).

Threshold (k = 10,000)	Edge count in the largest component	P
0.25	137	0.039
0.27	66	0.076
0.29	49	0.031
0.31	40	0.014
0.33	27	0.011
0.35	23	0.003
0.37	17	0.003
0.39	12	0.002
0.41	7	0.002
0.43	4	0.006
0.45	2	0.012

of voxels in the gastric network that overlapped with the voxels in the subnetwork we reported. Both maps were compared in MNI space. Defining the nodes for the Lausanne 2008 atlas (Hagmann et al., 2008) in MNI space was done by applying the parcellation scheme to the MNI template. Similarly, the same number of nodes were repeatedly (k = 10,000), randomly sampled and their overlap was again tested to determine a null reference distribution.

2.13. Temporal comparison between the subnetwork detected in the present study to Rebollo et al. (2018) gastric network

To quantify the temporal power spectrum from the BOLD signal time series we applied the multi-taper method (Thomson, 1982) to the preprocessed non-scrubbed fMRI signal. Multi-taper is a spectral estimation method that reduces the noise of the periodogram by averaging the spectrum over several windows (Thomson, 1982), and is considered less susceptible to noise compared to Naïve Fast Fourier Transform (Ghil et al., 2002). This was done on each resting-state run separately and was then averaged across the two runs. The analysis was performed using NiTime (Rokem et al., 2009), a Python open-source package for time-series analysis for neuroimaging data. The temporal analyses were conducted on the un-scrubbed data since one of the assumptions of the multi-taper method is that the data represent an uncensored continuous sample.

3. Results

3.1. Alterations in functional connectivity related to weight loss

First, we set to examine whether a subnetwork or a set of connected regions exists such that its within connectivity correlates with future weight loss. This was done by correlating each edge in the functional connectivity matrix with weight loss values across all subjects. As this analysis is conducted by examining whole-brain connectivity, it is critical to control for multiple comparisons. Hence, we utilized the Network-Based Statistic paradigm (NBS; Zalesky et al., 2010), that controls the FWER according to the detected subnetwork size. Using this approach, we found a significant subnetwork who's edges positively correlated with future weight loss. This subnetwork was evident across a wide range of thresholds indicating the robustness of this result ($z' = 0.25$, $0.29 \leq z' \leq 0.45$; all p's < 0.05; see Table 2). To exclude the specificity of these results to a particular preprocessing step, we reproduced this analysis and all the subsequent results with an alternative parcellation and time points censoring procedure (see Supplementary Sections 2 and 3). Weight loss was not correlated with age ($r(90) = 0.10$, $p = 0.32$), initial weight ($r(90) = -0.04$, $p = 0.72$) or BMI measured at baseline ($r(90) = 0.02$, $p = 0.86$). Additionally, the reported set of edges did not correlate with baseline BMI (mean correlation within the subnetwork; $r < 0.005$ for all thresholds). To provide a descriptive summary of the subnetwork composition, we examined the proportion of connections in the subnetwork to each of the 7 canonical resting-state networks reported by Yeo et al. (2011). The majority of this subnetwork (z' threshold = 0.25) was composed of connections to visual (32%) and somato-motor (24%) regions, along with connections to areas of the default (16%), ventral attention (11%) and limbic (8%) networks (Fig. 3; see Supplementary Section 1 for a detailed matrix). Interestingly, the bilateral pericalcarine was found as the node with the largest degree in this subnetwork across all threshold ($0.25 < z' < 0.43$). Thus, connectivity patterns of basic sensory and motor regions, rather than higher, multimodal regions, predict weight loss success following the intervention.

Controlling for potential confounds – movement and wakefulness state

Having documented the relation between functional connectivity and weight loss, it is critical to assess the possibility that these results might be accounted for by potential artifacts that are related to participants' movement or wakefulness state. Specifically, it could be that participants with higher self-control tended to move less or were more able to stay awake in the scanner as instructed, thus resulting in a different connectivity pattern (Tagliazucchi and Laufs, 2014; Van Dijk et al., 2012). Moreover, these participants may also better adhere to the dietary plan. Hence, we first examined the correlation between participants' in-scanner movement parameters and their weight loss values. Importantly, weight loss was not correlated with the mean absolute translation (x, y, z) or rotation (pitch, yaw, roll) in any of the 6 axes (all $r(90) < 0.08$, all p-values > 0.28). Next, although wakefulness levels were not directly measured, we used a previously suggested marker of early sleep stage to assess in-scanner wakefulness. Specifically, several studies reported a dramatic increase in whole-brain connectivity during light sleep (Spoormaker et al., 2010; Tagliazucchi and Laufs, 2014). Hence, we examined the mean connectivity across all ROIs and found no correlation with future weight loss ($r(90) = 0.04$, $p = 0.71$). Moreover, the absence of correlation between in-scanner head motion, previously associated with sleep (Curtis et al., 2016; Spoormaker et al., 2010), and weight loss further precludes vigilance levels as a possible confounding factor.

3.2. Predicting future weight loss using Connectome-based Predictive Modeling (CPM) and Leave-One-Out cross-validation

A connectivity-based prediction model can allow us to assess the extent to which brain connectivity patterns at baseline can predict future weight loss, as opposed to reporting mere significant differences in connectivity. Importantly, using cross-validation we can gain an empirical estimation of such a model to generalize its prediction to a novel set of subjects. Accordingly, we utilized the CPM protocol (Shen et al., 2017; see Section 2.9.) to test the extent to which weight loss can be predicted from the functional connectivity matrix. Using Leave-One-Out cross-validation (LOO-CV), across a wide range of thresholds (0.25, 0.26,…,0.35) 4.31–10.60% of the weight loss variability (mean = 8.14%; Fig. 4) could be accounted for by the model. To test for a possible effect of intervention group we correlated percent weight loss with the mean edge value within the weight loss related network ($z' > 0.25$) for all three intervention groups. This effect was similar across all three groups ($r(26) = 0.54$, $r(26) = 0.63$, $r(32) = 0.61$; all p's < 0.003; for groups PA,PA+MED and PA+MED+ polyphenol respectively; Supplementary Fig. 12). This further highlights the robustness of resting-state connectivity as a future weight loss predictor.

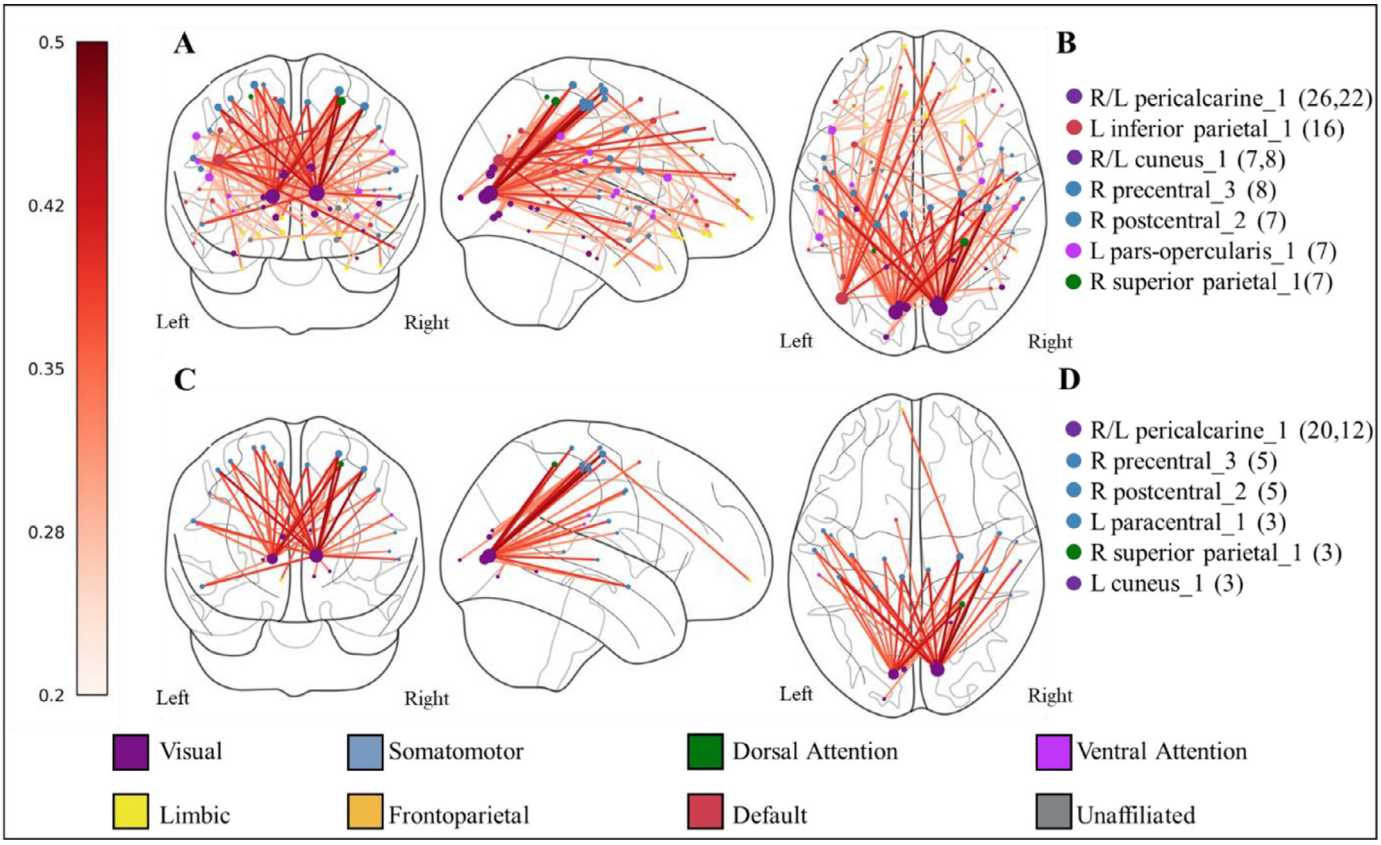

Fig. 3. The subnetwork detected with the NBS procedure which identifies a set of connected edges whose strength correlates with future weight loss. Coronal, sagittal and axial projected graph representation depicting the nodes and edges of the weight loss related subnetwork. In the NBS procedure, a subnetwork is comprised of edges whose correlation with a given value (i.e., weight loss) is higher than a certain threshold. Accordingly, the subnetwork is presented for a correlation threshold of $z' > 0.25$ (A) and $z' > 0.31$ (C). Node degree (i.e. the number of existing connections for a given node) is represented by the node size. The correlation magnitude of each edge with weight loss is represented by the edge color. Edges' color scale bar is shown on the left. (B) and (D) shows a list of nodes with the highest degree for the $z' > 0.25$ (B) and $z' > 0.31$ (D) thresholds. Nodes degree is specified in brackets and the number next to the node's name indicates its sub-parcellation in the Lausanne 2008 atlas (Hagmann et al., 2008). Nodes' color represents their affiliation to one of the 7 canonical resting-state networks according to Yeo's et al. (2011).

3.3. The relation between behavioral measurements of executive function and subsequent weight loss

In line with the inhibitory control hypothesis of weight regulation, we wanted to test the role of executive functions in RSFC correlates of future weight loss. A basic analysis of the executive functions data was conducted for a hundred and eighty-two subjects (see Section 2.10 for exclusion criteria). A further, detailed analysis of the executive function behavioral data is the focus of a separate study from the same research group and hence reported here only in relation to the functional connectivity analysis (Kaplan et al., Manuscript in preparation). We found a modest, but significant correlation between the general executive functions score and weight loss ($r(180) = 0.21$, $P = 0.005$). As expected (Wasylyshyn et al., 2011) all executive function measurements were negatively correlated with age ($r(180) = -0.41, -0.16, -0.38$ all p's < 0.05; for inhibition, switching and working memory respectively). Therefore, we additionally examined the correlation between the general executive function scores and weight loss after regressing out subjects' age and found that the significant correlation was maintained ($r(180) = 0.25$, $P < 0.001$). Given the well-documented correlation of executive functions with age (Salthouse, 2005; Verhaeghen, 2011), it is noteworthy that executive function variability that is independent of age predicts future weight loss. In subsequent analyses, we decided to focus on this component of executive function variability, hence the following analyses were conducted on the age-controlled executive function scores. Next, we tested the relation of each of the three executive function measures to future weight loss. We found a significant correlation with the inhibition and switching measures ($r(180) = 0.23$, $p = 0.002$; $r(180) = 0.21$, $p = 0.005$; respectively), but not with the working memory measure ($r(180) = 0.13$, $p = 0.09$), although these differences do not allow us to conclude which exact executive function factor underlies the effect. Given the correlation of behavioral executive function measures with weight loss, in the following paragraph we test whether the detected subnetwork relates to executive function abilities and compare these measures' ability to predict future weight loss.

3.4. Relation between weight loss, connectivity patterns and performance on executive function tasks

Next, to similarly assess the predictive value of executive function as a subsequent weight loss predictor, we used a linear regression model evaluated with leave-one-out cross-validation (LOO-CV). Explained variance of general executive function, inhibition, switching, and working memory was 2.15%, 3.02%, 2.05% and −0.02% respectively (Fig. 4). Explained variance across all connectivity-based model thresholds was higher than the best behavioral predictor, although this comparison should be taken with caution due to the different measures, statistical procedures and available sample size. Next, we wanted to examine whether executive function may underlie the observed resting-state connectivity correlates of future weight loss. To do so, we repeated the CPM procedure after regressing out general executive function scores from each edge in the connectivity matrix. Importantly, after controlling for executive function, the connectivity-based model explained a larger portion of the weight loss variance (0.25, 0.26,…,0.35;

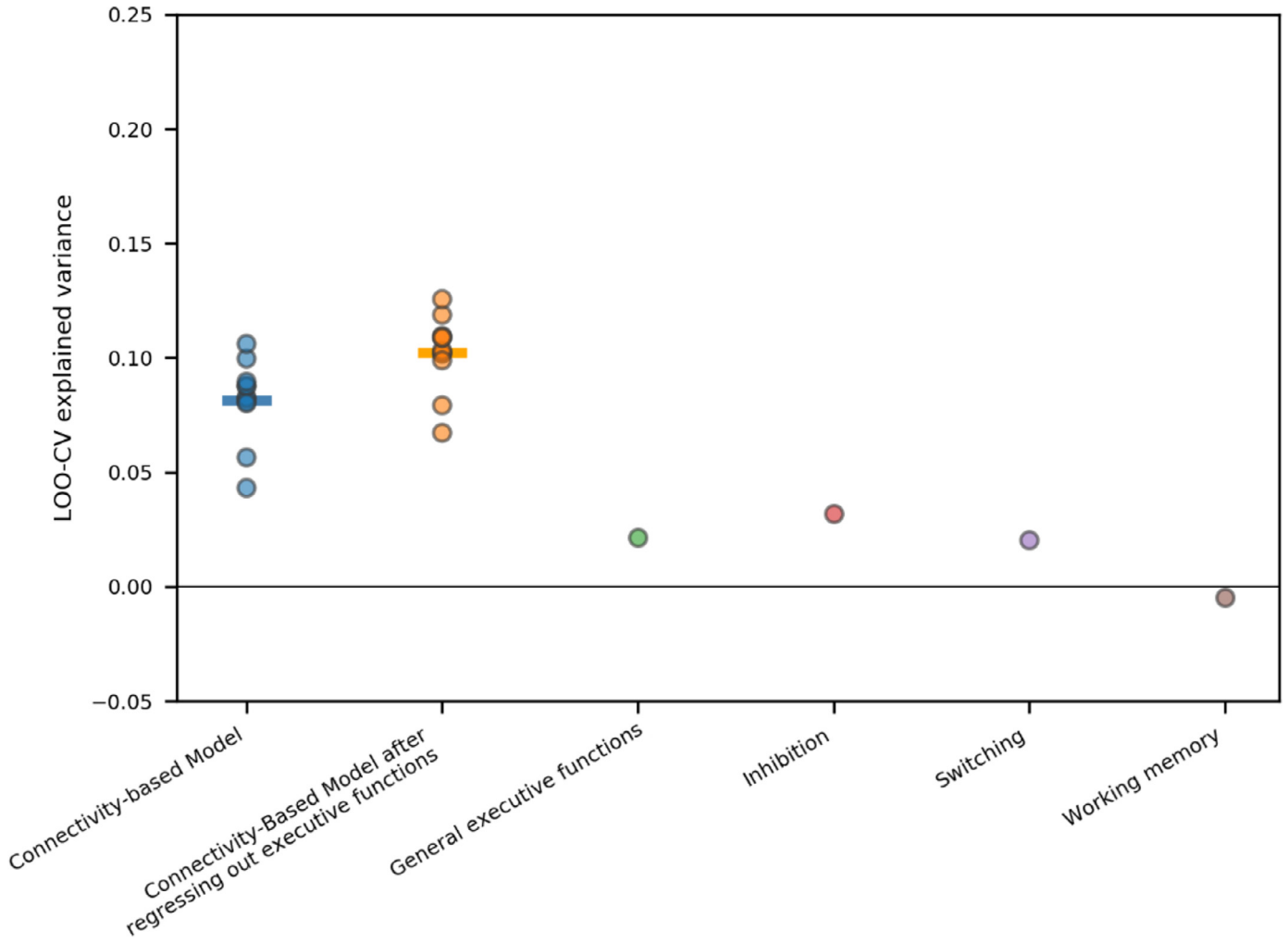

Fig. 4. Explained variance of different weight loss predictors, as evaluated with a leave one out cross-validation procedure. In the connectivity-based models' predictions (2 leftmost columns on the graph), each point indicates a different threshold level (0.25, 0.26,…,0.35), and the vertical lines represent the mean over all thresholds.

6.72–12.56%; mean = 10.21%; Fig. 4). Therefore, high executive function abilities did not account for the relation of connectivity patterns within the subnetwork to future weight loss.

3.5. Comparing the subnetwork detected with NBS to Rebollo et al. (2018) gastric network

Rebollo et al. (2018) recently reported that a set of regions, mainly primary and secondary sensory cortices, were significantly correlated with gastric slow-wave electrical activity (0.05 Hz). Interestingly, the weight loss related subnetwork we report here, show some spatial, anatomical overlap with the gastric network reported by Rebollo et al. (2018) (Fig. 5). Given these findings, we wanted to quantify the spatial similarity of the subnetwork we report here which is related to weight-loss and the gastric network directly measured by Robollo and colleagues (Robollo et al., 2018). Furthermore, we wanted to examine whether cortical oscillations in the gastric electrical rhythm (0.05 Hz), previously reported in the literature, are related to future weight loss. The NBS procedure does not test the significance of individual edges, but rather, the significance of the network as a whole. Hence, we should assume that certain edges in the network are false positive. For this reason, in the following analysis, we spatially restricted our weight loss related subnetwork only to nodes with high degree (Q1, degree ≥ 4) using the lowest NBS threshold ($z' > 0.25$).

3.5.1. Quantifying the similarity at the spatial domain between the subnetwork detected in the present study to Rebollo et al. (2018) gastric network

The subnetwork found in the present study and the gastric network described in Rebollo et al. (2018), differ in many ways, such as the definition of the two networks, the different methodological approaches by which they were defined, their respective populations and the spatial definition methods (voxel-wise/anatomical pre-defined ROIs). Yet, we wanted to examine the extent of the similarity between these two networks (Fig. 5). Specifically, we measured the percent of voxels in Rebollo et al. (2018) network that overlapped with the weight loss related subnetwork. To evaluate the statistical significance of the results, we compared them to a null distribution of randomly selected sets of regions from the same parcellation (see Section 2.12.). The percent overlap was higher than any randomly selected set of regions (k = 10,000, empirical percent overlap = 18.7%, $p < 0.0001$; see Fig. 6).

3.5.2. Quantifying the similarity at the temporal domain between the subnetwork detected in the present study to Rebollo et al. (2018) gastric network

We tested whether power in the stomach basal electrical rhythm (0.05 Hz) within the subnetwork we found, would be correlated with weight loss. Critically, we found a modest, yet significant negative correlation between power in 0.05 Hz and future weight loss ($r(90) = -0.27$,

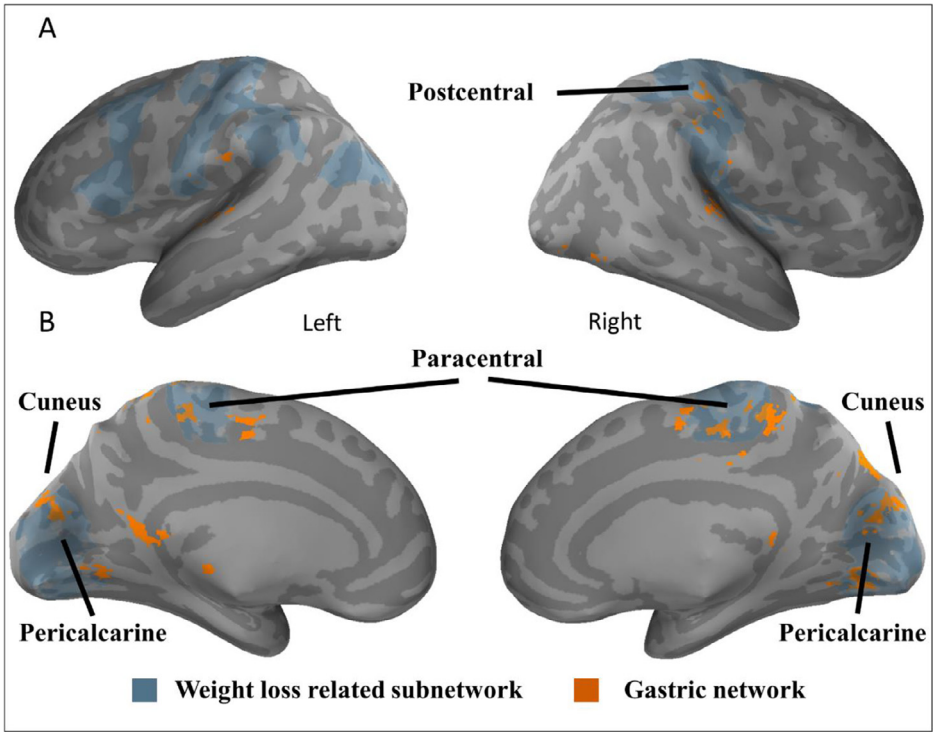

Fig. 5. Projection of the two networks on an inflated cortical surface of the right and left hemispheres. The surface is presented in lateral (A) and medial (B) views. Blue indicates the weight loss related subnetwork (half transparent), and orange indicates Rebollo et al. (2018) gastric network. The annotations, defined using the labels of the 128 nodes Lausanne 2008 atlas (Hagmann et al., 2008), indicate anatomical overlapping areas.

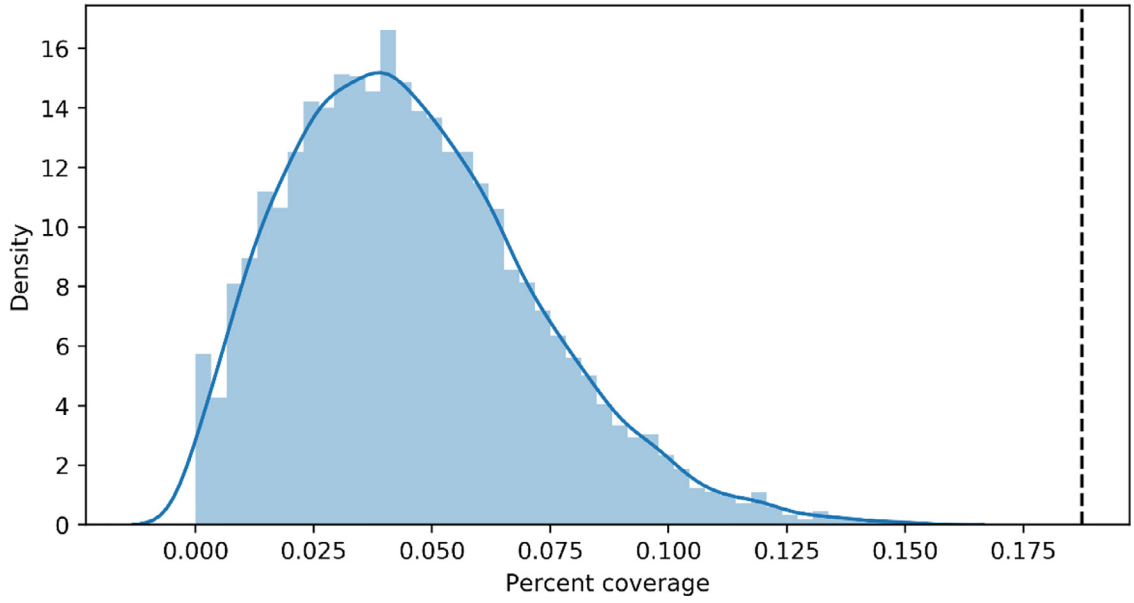

Fig. 6. Distribution of the spatial overlap to Rebollo's et al. (2018) gastric network of random network permutations (k= 10,000). Spatial overlap was measured as percent coverage of the gastric network. The vertical black dotted line represents the empirical overlap of the weight loss related network we reported to the gastric network, this value was higher than for any network permutation.

$p = 0.008$; Fig. 7). The correlation was specific to the weight loss related subnetwork when tested against a set of random networks with the same number of nodes with a matched size (k = 10,000; p = 0.012). Importantly, testing the correlation of power and weight loss values across the frequencies of the resting-state relevant spectrum (0.1–0.01 Hz) revealed a peak in 0.0475 Hz (Fig. 8), implying the specificity of this finding to the stomach basal electrical rhythm. Hence, the correlation of the measured power and future weight loss is specific to both our detected subnetwork and the gastric frequency.

4. Discussion

4.1. The weight loss related subnetwork

In the current work, we examined the potential correlation between resting-state functional connectivity patterns and successful weight loss following a lifestyle intervention. Resting-state functional connectivity and weight of 92 participants were measured at baseline and their subsequent weight loss was assessed after 6 months of a lifestyle intervention.

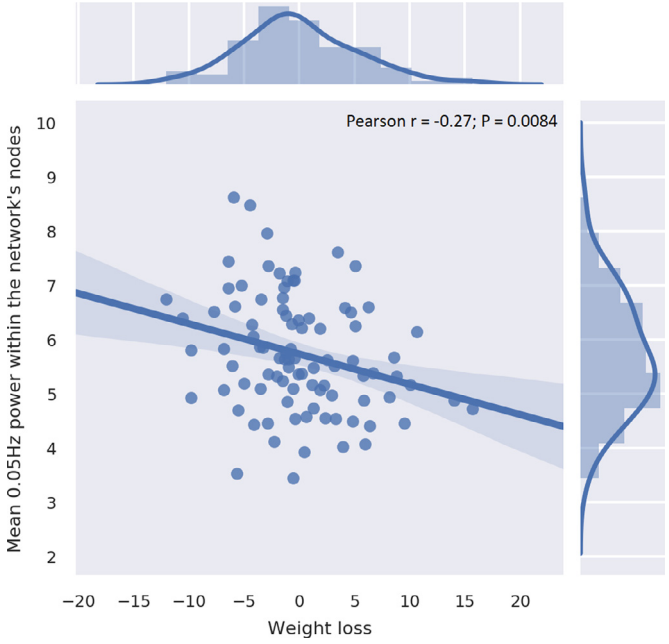

Fig. 7. Regression plot of future weight loss compared to the mean calculated power in the stomach basal electrical frequency (0.05 Hz) within the weight loss related subnetwork. Weight loss is the percent weight loss value after regressing out the effect of the intervention group. The weight loss values are centered around zero due to regressing out of the group effect. The Pearson correlation coefficient and the *p*-value are indicated on the top right side of the plot. The top and right panels of the figure depict histograms and kernel density plots of the distribution of the weight loss and the mean 0.05 Hz power (respectively).

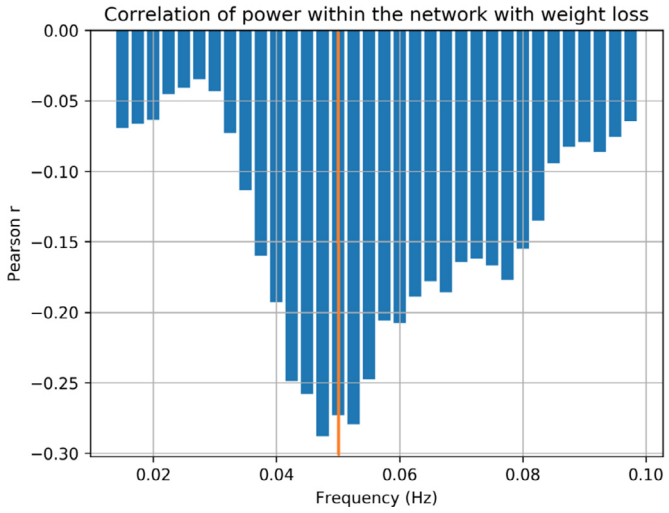

Fig. 8. Correlation between future weight loss (standardized values) and the mean calculated power within the weight loss related subnetwork across the resting-state relevant spectrum (0.1–0.01 Hz). The vertical orange line indicates the stomach basal electrical activity (0.05 Hz). As is evident, the peak of the distribution of the power of the subnetwork reported here overlaps with the basal electrical activity as reported in the literature.

In line with previous studies demonstrating the significance of executive function abilities to success in a dietary weight loss intervention (Gettens and Gorin, 2017), subjects were also administered an executive function assessment battery (Gordon et al., 2018). Using the NBS procedure, we identified a robust functional subnetwork that was composed of edges positively correlated with future weight loss. Next, using the connectivity-based prediction model method (CPM; Shen et al., 2017), we quantified the extent to which a simple univariate model, based on connectivity patterns within this subnetwork, could predict future weight loss. Thus, demonstrating that these findings are also replicable using cross-validation. While edges in this subnetwork correlated with weight loss, they surprisingly did not correlate with baseline BMI. This may be due to range restriction since all participants were initially overweight or obese. Importantly, weight loss was not correlated with in-scanner movement parameters or with global connectivity, which is considered a within scanner sleep biomarker (Spoormaker et al., 2010; Tagliazucchi and Laufs, 2014).

4.2. Resting-state connectivity correlates of future weight loss and neural theories of weight regulation

As noted in the Introduction, there are three prominent neural theories that may underlie impaired weight regulation (Stice and Yokum, 2016). These include: 1. Over-sensitivity to palatable food cues; 2. A deficit in inhibitory control and 3. Abnormal reward processing. Of these, the abnormal reward theory suggests that increased reward response to food consumption subsequently leads to over-eating. In line with this theory, we expected baseline connectivity in reward-related brain regions to account for future weight loss. In contrast, most of the cortical connections in our reported weight loss related subnetwork were to nodes of visual or somato-motor resting-state networks (Yeo et al., 2011). Notably, the bilateral pericalcarine, the anatomical location of the primary visual cortex, was the node with the highest degree within this subnetwork. Similarly, these findings do not easily converge with the impaired inhibitory control theory, which highlights the role of cortical areas related to executive functions (e.g. DLPFC) in successful weight reduction (Dong et al., 2015). Moreover, regressing out general executive function behavioral scores from each edge in the connectivity matrix, thus eliminating the contribution of executive functions from the connectivity variance, actually improved the ability of the network-based model to account for future weight loss. Interestingly, executive function behavioral measures had a moderate correlation with future weight loss. This may imply that despite the apparent role of executive function in successful weight loss, this relation could not be easily captured using RSFC. The significant role of sensory cortical regions within this subnetwork might coincide with the theory of over-sensitivity for palatable food cues. Indeed, similar findings were observed in perceptual experiments while participants were presented with visual or olfactory stimuli of food (Stice and Burger, 2019). Despite the absence of food-related stimuli in the present study, we suggest that the observed involvement of sensory areas may also be due to contextual influence of the awareness to the planned dietary intervention or the mandatory fasting before the examination (2 h). However, previous RSFC studies related increased connectivity within the saliency network, rather than sensory or motor networks, to impaired weight regulation. Increased connectivity within the saliency network supposedly underlies increased baseline susceptibility to food cues in obesity (García-García et al., 2013; Sewaybricker et al., 2019). Hence, in the following paragraph, we consider and test an additional post-hoc hypothesis regarding a role of brain-gastric interaction to account for these neural findings.

4.3. Possible role of stomach-brain connectivity in the weight loss related subnetwork

As an attempt to account for our unexpected findings, we conducted an additional, post-hoc analysis. This analysis stemmed from recent studies which implicated that a network of cortical regions, mainly including somatosensory, motor and visual areas, that was measured using resting-state fMRI, show synchrony with the stomach slow-wave electrical activity (Rebollo et al., 2018; Richter et al., 2017). This electrical activity, peaking at 0.05 Hz, is generated by the intestine cells of Cajal, and coordinates waves of muscle contractions that travel the stomach and promote both digestion and emptying of the gastric content (Grundy and

Brookes, 2011). Notably, gastric motility is considered an important mediator of hunger and satiety and hence, we hypothesized that this factor might also be related to weight loss (Janssen et al., 2011). To explore this hypothesis, we examined the spatial and temporal similarity between the weight loss subnetwork we discovered in the present study and the gastric network reported by Rebollo et al. (2018). We found a modest, yet significant spatial overlap between the two networks, even though they were obtained using very different methodological approaches, populations, and node definition schemes. Furthermore, frequency analysis revealed that the 0.05 Hz power, which is the gastric basal frequency, was negatively correlated with future weight loss in the nodes of the subnetwork obtained in the present study. Importantly, this correlation of the frequency of hemodynamic fluctuations, and future weight loss success was specific to the weight loss subnetwork and to the specific 0.05 Hz basal electrical gastric frequency. Establishing the prominence of brain-gastric communication in successful weight reduction would require direct recording of the gastric activity in a similar study. Nevertheless, in this work, we provided preliminary evidence for the plausibility of the involvement of this subnetwork in successful weight loss.

4.4. Gastric signaling to the cortex

The hypothesis regarding the involvement of brain-gastric communication in the subnetwork we discovered in the present study must be supported by known anatomical pathways. Respectively, several studies have reported the existence of indirect anatomical connections from the stomach to these sensory regions and their reactivity to gastric stimulation. For example, the primary and secondary somato-sensory cortices and the insula are known to receive gastric inputs mostly via the vagus nerve (Grundy, 2002; Grundy and Brookes, 2011). Vagal afferents typically relay mechanical information regarding stretch or distension of the stomach (Ozaki et al., 1999), an indicator of the stomach volume. Vagal afferents originated from the stomach project to the nucleus of the solitary tract (NTS), which innervates mostly the parabrachial nucleus (PBN). Among others, the PBN sends projections to ventro-posterior thalamus that in turn, projects to cortical regions such as the primary and secondary somato-sensory cortices and the insula (Mayer et al., 2006). Consistently with this pattern of anatomical connections, the insula, somatosensory and motor regions, that we found in the present study as part of the weight loss related subnetwork, are associated in the literature with gastric stimulation, as seen for example in fMRI brain activation following gastric distention (Wang et al., 2008). Moreover, areas such as the pericalcarine, cuneus and lateral occipital cortex, that are typically associated with visual function, also respond to gastric stimulation as evident in multiple imaging studies (Cao et al., 2019; Pigarev et al., 2006; Rebollo et al., 2018; Van Oudenhove et al., 2009). These findings may explain the prominence of visual regions in our detected subnetwork. Similarly, the fusiform gyrus and the cuneus were found to respond to the stomach nutrient content and suggested to be involved in evaluating reward aspects of these signals (DiFeliceantonio et al., 2018; Little et al., 2014). This could be accounted for by evidence indicating the existence of major afferent inputs from the PBN to the lateral geniculate nucleus (LGN), even though the latter is considered a visual thalamic relay nucleus (Guillery and Sherman, 2002). Relatedly, single-cell recordings in sleeping cats documented that simple and complex V1 cells respond to gastric stimulation (Pigarev, 1994). Finally, differences in cortical reactivity to gastric distention were found among obese subjects (Tomasi et al., 2009), thus indicating the possible relevance of gastric-brain interaction for body weight regulation.

4.5. Limitations

It is important to consider the limitations of the study. First, the gender distribution (F: 11, M: 81; F:12%, M: 88%), reflecting the workplace profile from which participants were recruited, misrepresents the proportion of obese women within the general population (F: 51%, M: 49%; CDC, 2018). The low number of female participants does not allow to model gender effect on functional connectivity and weight loss relations. Thus, inference from the current work to the general population should be done with cautious. Secondly, we interpreted our results regarding the weight loss related subnetwork considering existing neural theories of weight regulation (Stice and Yokum, 2016). This was done in light of the behavioral executive function measures and the subnetwork's edges and nodes composition. Among the three neural theories, we reported a moderate support for the over-sensitivity for palatable food cues theory. Nevertheless, this should be further corroborated by directly combining behavioral measures of food cues sensitivity. Finally, a direct gastric activity recording would allow us to best address our post-hoc hypothesis regarding the role of brain-gastric interaction in weight loss. It is important that such recordings would be combined with neural or gastric stimulation to establish the origin and directionality of this interaction. Notably, in the present study, we only examined this hypothesis by testing spatial and temporal similarities to a previously reported cortical network synchronized with the gastric activity (Rebollo et al., 2018).

4.6. Conclusions

In this work, we found evidence of a brain subnetwork supporting successful weight loss. Connectivity within this subnetwork, comprised mostly of connections to cortical sensory and motor regions, predicted dietary success in weight loss after 6 months of lifestyle intervention. While weight loss was positively correlated with executive function behavioral measures, we have shown that connectivity within this subnetwork is not likely to relate to executive function abilities. Similarly, the involvement of basic sensory and motor cortical regions do not easily coincide with the abnormal reward theory. The involvement of sensory regions in this subnetwork might provide evidence in favor of the over-sensitivity to food cues theory, although similar findings were typically reported in experiments in which visual or olfactory stimuli of food were presented (Stice and Burger, 2019). Rather, we documented some evidence indicating that these connectivity patterns may arise from brain-gastric interactions. We note though that such evidence should be further addressed and confirmed by directly recording the electrical activity from the stomach in a future study. These findings may have an important implication for our understanding of the etiology of obesity and the mechanism of response to dietary intervention.

CRediT authorship contribution statement

Gidon Levakov: Conceptualization, Methodology, Investigation, Formal analysis, Software, Visualization, Writing - original draft, Writing - review & editing. **Alon Kaplan:** Investigation, Project administration, Writing - review & editing. **Anat Yaskolka Meir:** Investigation, Project administration. **Ehud Rinott:** Investigation, Project administration. **Gal Tsaban:** Investigation, Project administration. **Hila Zelicha:** Investigation, Project administration. **Nachshon Meiran:** Conceptualization, Methodology, Writing - review & editing. **Ilan Shelef:** Resources, Conceptualization, Methodology, Writing - review & editing. **Iris Shai:** Resources, Conceptualization, Methodology, Supervision, Funding acquisition, Writing - review & editing. **Galia Avidan:** Conceptualization, Methodology, Writing - original draft, Writing - review & editing, Supervision.

Data availability

The un-threshold edge-wise correlation matrices of functional connectivity and future weight loss for all three preprocessing alternatives and the preprocessing C-PAC configuration file are available at https://doi.org/10.6084/m9.figshare.c.4557347.v1. The

main NBS analysis code is available at https://github.com/GidLev/NBS-correlation.

Acknowledgments

This work was supported by grants from: The Deutsche Forschungsgemeinschaft (DFG, German Research Foundation) – Projektnummer 209933838 – SFB 1052; the DFG, Obesity Mechanisms; Israel Ministry of Health (grant no. 87472511), Israel Ministry of Science and Technology (grant 3-13604), and the California Walnuts Commission.

Supplementary materials

Supplementary material associated with this article can be found, in the online version, at doi:10.1016/j.neuroimage.2020.117403.

References

Behzadi, Y., Restom, K., Liau, J., Liu, T.T., 2007. A component based noise correction method (CompCor) for BOLD and perfusion based fMRI. NeuroImage 37 (1), 90–101. doi:10.1016/j.neuroimage.2007.04.042.

Birn, R.M., Molloy, E.K., Patriat, R., Parker, T., Meier, T.B., Kirk, G.R., …, Prabhakaran, V., 2013. The effect of scan length on the reliability of resting-state fMRI connectivity estimates. NeuroImage 83, 550–558. doi:10.1016/J.NEUROIMAGE.2013.05.099.

Boly, M., Balteau, E., Schnakers, C., Degueldre, C., Moonen, G., Luxen, A., …, Laureys, S., 2007. Baseline brain activity fluctuations predict somatosensory perception in humans. Proc. Natl. Acad. Sci. 104 (29), 12187–12192. doi:10.1073/pnas.0611404104.

Bullmore, E., Sporns, O., 2009. Complex brain networks: Graph theoretical analysis of structural and functional systems. Nature Reviews Neuroscience. Nature Publishing Group doi:10.1038/nrn2575.

Burger, K.S., Stice, E., 2013. Elevated energy intake is correlated with hyperresponsivity in attentional, gustatory, and reward brain regions while anticipating palatable food receipt. Am. J. Clin. Nutr. 97 (6), 1188–1194. doi:10.3945/ajcn.112.055285.

Cameron, C., Sharad, S., Brian, C., Ranjeet, K., Satrajit, G., Chaogan, Y., …, Michael, M., 2013. Towards automated analysis of connectomes: the configurable pipeline for the analysis of connectomes (C-PAC). Neuroinformatics 7. doi:10.3389/conf.fninf.2013.09.00042.

Cao, J., Lu, K.-H., Oleson, S.T., Phillips, R.J., Jaffey, D., Hendren, C.L., …, Liu, Z., 2019. Gastric stimulation drives fast BOLD responses of neural origin. NeuroImage 197, 200–211. doi:10.1016/J.NEUROIMAGE.2019.04.064.

CDC. (2018). Nutrition, Physical Activity, and Obesity: Data, Trends and Maps | DNPAO | CDC. Retrieved December 26, 2019, from https://www.cdc.gov/nccdphp/dnpao/data-trends-maps/index.html

Contreras-Rodríguez, O., Martín-Pérez, C., Vilar-López, R., Verdejo-Garcia, A., 2017. Ventral and dorsal striatum networks in obesity: link to food craving and weight gain. Biol. Psychiatry 81 (9), 789–796. doi:10.1016/J.BIOPSYCH.2015.11.020.

Cummings, D.E., Overduin, J., 2007. Gastrointestinal regulation of food intake. J. Clin. Invest. 117 (1), 13–23. doi:10.1172/JCI30227.example.

Curtis, B.J., Williams, P.G., Jones, C.R., Anderson, J.S., 2016. Sleep duration and resting fMRI functional connectivity: examination of short sleepers with and without perceived daytime dysfunction. Brain Behav. 6 (12), e00576. doi:10.1002/brb3.576.

D'Archivio, M., Filesi, C., Varì, R., Scazzocchio, B., Masella, R., 2010. Bioavailability of the polyphenols: status and controversies. Int. J. Mol. Sci. doi:10.3390/ijms11041321.

Daducci, A., Gerhard, S., Griffa, A., Lemkaddem, A., Cammoun, L., Gigandet, X., …, Thiran, J.P., 2012. The connectome mapper: an open-source processing pipeline to map connectomes with MRI. PLoS One 7 (12), e48121. doi:10.1371/journal.pone.0048121.

de Araujo, I.E., Oliveira-Maia, A.J., Sotnikova, T.D., Gainetdinov, R.R., Caron, M.G., Nicolelis, M.A.L., Simon, S.A., 2008. Food reward in the absence of taste receptor signaling. Neuron 57 (6), 930–941. doi:10.1016/j.neuron.2008.01.032.

DiFeliceantonio, A.G., Coppin, G., Rigoux, L., Edwin Thanarajah, S., Dagher, A., Tittgemeyer, M., Small, D.M., 2018. Supra-additive effects of combining fat and carbohydrate on food reward. Cell Metab. 28 (1), 33–44. doi:10.1016/J.CMET.2018.05.018.

Dong, D., Jackson, T., Wang, Y., Chen, H., 2015. Spontaneous regional brain activity links restrained eating to later weight gain among young women. Biol. Psychol. 109, 176–183. doi:10.1016/j.biopsycho.2015.05.003.

Finn, E.S., Shen, X., Scheinost, D., Rosenberg, M.D., Huang, J., Chun, M.M., …, Constable, R.T., 2015. Functional connectome fingerprinting: identifying individuals using patterns of brain connectivity. Nat. Neurosci. 18 (11), 1664–1671. doi:10.1038/nn.4135.

Fischl, B., Sereno, M.I., Dale, A.M., 1999. Cortical surface-based analysis: II. Inflation, flattening, and a surface-based coordinate system. NeuroImage. Academic Press doi:10.1006/nimg.1998.0396.

Fischl, B., Van Der Kouwe, A., Destrieux, C., Halgren, E., Ségonne, F., Salat, D.H., …, Dale, A.M., 2004. Automatically parcellating the human cerebral cortex. Cereb. Cortex 14 (1), 11–22. doi:10.1093/cercor/bhg087.

Friedman, N.P., Miyake, A., 2017. Unity and diversity of executive functions: individual differences as a window on cognitive structure. Cortex 86, 186–204. doi:10.1016/J.CORTEX.2016.04.023.

García-García, I., Jurado, M.Á., Garolera, M., Segura, B., Sala-Llonch, R., Marqués-Iturria, I., …, Junqué, C., 2013. Alterations of the salience network in obesity: a resting-state fMRI study. Hum. Brain Mapp. 34 (11), 2786–2797. doi:10.1002/hbm.22104.

Geha, P.Y., Aschenbrenner, K., Felsted, J., O'Malley, S.S., Small, D.M., 2013. Altered hypothalamic response to food in smokers. Am. J. Clin. Nutr. 97 (1), 15–22. doi:10.3945/ajcn.112.043307.

Gettens, K.M., Gorin, A.A., 2017. Executive function in weight loss and weight loss maintenance: a conceptual review and novel neuropsychological model of weight control. J. Behav. Med. doi:10.1007/s10865-017-9831-5, Springer US, https://doi.org/.

Ghil, M., Allen, M.R., Dettinger, M.D., Ide, K., Kondrashov, D., Mann, M.E., …, Yiou, P., 2002. Advanced spectral methods for climatic time series. Rev. Geophys. 40 (1), 1003. doi:10.1029/2000RG000092.

Gordon, S., Todder, D., Deutsch, I., Garbi, D., Neuropsychologia, N.G.-, 2018. In: Are Resting State Spectral Power Measures Related to Executive Functions in Healthy Young Adults?, 108. Elsevier, pp. 61–72 Retrieved from.

Gorgolewski, K., Burns, C.D., Madison, C., Clark, D., Halchenko, Y.O., Waskom, M.L., Ghosh, S.S., 2011. Nipype: a flexible, lightweight and extensible neuroimaging data processing framework in python. Front. Neuroinform. 5, 13. doi:10.3389/fninf.2011.00013.

Grundy, D., 2002. Neuroanatomy of visceral nociception: vagal and splanchnic afferent. Gut 51 (Supplement 1), i2–i5. doi:10.1136/gut.51.suppl_1.i2.

Grundy, David, Brookes, S, 2011. Neural control of gastrointestinal function. Colloq. Ser. Integr. Syst. Physiol.: Mol. Funct. 3 (9), 1–134. doi:10.4199/C00048ED1V01Y201111ISP030.

Guillery, R.W., Sherman, S.M., 2002. Thalamic Relay functions and their role in corticocortical communication: generalizations from the visual system. Neuron 33 (2), 163–175. doi:10.1016/s0896-6273(01)00582-7.

Hagmann, P., Cammoun, L., Gigandet, X., Meuli, R., Honey, C.J., Van Wedeen, J., Sporns, O., 2008. Mapping the structural core of human cerebral cortex. PLoS Biol. 6 (7), 1479–1493. doi:10.1371/journal.pbio.0060159.

Han, J.E., Boachie, N., Garcia-Garcia, I., Michaud, A., Dagher, A., 2018. Neural correlates of dietary self-control in healthy adults: a meta-analysis of functional brain imaging studies. Physiol. Behav. 192, 98–108. doi:10.1016/J.PHYSBEH.2018.02.037.

Janssen, P., Vanden Berghe, P., Verschueren, S., Lehmann, A., Depoortere, I., Tack, J., 2011. Review article: the role of gastric motility in the control of food intake. Alimentary Pharmacology and Therapeutics. WileyBlackwell (10.1111), https://doi.org/doi:10.1111/j.1365-2036.2011.04609.x.

Kaplan, A., Levakov, G., Yaskolka Meir, A., Rinott, E., Tsaban, G., Zelicha, H., … Avidan, G. (2019). Executive Functions Predicts Future Weight Loss: A Prospective Study. Manuscript in Preparation.

Kroemer, N.B., Sun, X., Veldhuizen, M.G., Babbs, A.E., de Araujo, I.E., Small, D.M., 2016. Weighing the evidence: variance in brain responses to milkshake receipt is predictive of eating behavior. NeuroImage 128, 273–283. doi:10.1016/J.NEUROIMAGE.2015.12.031.

Lavagnino, L., Arnone, D., Cao, B., Soares, J.C., Selvaraj, S., 2016. Inhibitory control in obesity and binge eating disorder: a systematic review and meta-analysis of neurocognitive and neuroimaging studies. Neurosci. Biobehav. Rev. 68, 714–726. doi:10.1016/J.NEUBIOREV.2016.06.041.

Lerman-Sinkoff, D.B., Sui, J., Rachakonda, S., Kandala, S., Calhoun, V.D., Barch, D.M., 2017. Multimodal neural correlates of cognitive control in the Human Connectome Project. NeuroImage 163, 41–54. doi:10.1016/J.NEUROIMAGE.2017.08.081.

Little, T.J., McKie, S., Jones, R.B., D'Amato, M., Smith, C., Kiss, O., …, McLaughlin, J.T., 2014. Mapping glucose-mediated gut-to-brain signalling pathways in humans. NeuroImage 96, 1–11. doi:10.1016/J.NEUROIMAGE.2014.03.059.

MacLean, P.S., Rothman, A.J., Nicastro, H.L., Czajkowski, S.M., Agurs-Collins, T., Rice, E.L., …, Loria, C.M., 2018. The accumulating data to optimally predict obesity treatment (ADOPT) core measures project: rationale and approach. Obesity 26, S6–S15. doi:10.1002/oby.22154.

Mayer, E.A., Naliboff, B.D., Craig, A.D.B., 2006. Neuroimaging of the brain-gut axis: from basic understanding to treatment of functional GI disorders. Gastroenterology 131 (6), 1925–1942. doi:10.1053/j.gastro.2006.10.026.

Mokdad, A.H., Serdula, M.K., Dietz, W.H., Bowman, B.A., Marks, J.S., Koplan, J.P., 1999. The spread of the obesity epidemic in the United States, 1991–1998. JAMA 282 (16), 1519. doi:10.1001/jama.282.16.1519.

Mokhtari, F., Rejeski, W.J., Zhu, Y., Wu, G., Simpson, S.L., Burdette, J.H., Laurienti, P.J., 2018. Dynamic fMRI networks predict success in a behavioral weight loss program among older adults. NeuroImage 173, 421–433. doi:10.1016/J.NEUROIMAGE.2018.02.025.

Neseliler, S., Hu, W., Larcher, K., Zacchia, M., Dadar, M., Scala, S.G., …, Dagher, A., 2019. Neurocognitive and hormonal correlates of voluntary weight loss in humans. Cell Metabol. 29 (1), 39–49. doi:10.1016/J.CMET.2018.09.024.

Nomi, J.S., Vij, S.G., Dajani, D.R., Steimke, R., Damaraju, E., Rachakonda, S., …, Uddin, L.Q., 2017. Chronnectomic patterns and neural flexibility underlie executive function. NeuroImage 147, 861–871. doi:10.1016/j.neuroimage.2016.10.026.

Ozaki, N., Sengupta, J.N., Gebhart, G.F., 1999. Mechanosensitive properties of gastric vagal afferent fibers in the rat. J. Neurophysiol. 82 (5), 2210–2220. doi:10.1152/jn.1999.82.5.2210.

Pang, J., Zhang, Z., Zheng, T.Z., Bassig, B.A., Mao, C., Liu, X., …, Peng, Y., 2016. Green tea consumption and risk of cardiovascular and ischemic related diseases: a meta-analysis. Int. J. Cardiol. 202, 967–974. doi:10.1016/j.ijcard.2014.12.176.

Park, M.I., Camilleri, M., 2005. Gastric motor and sensory functions in obesity. Obesity Research. Wiley-Blackwell doi:10.1038/oby.2005.51.

Pigarev, I., Almirall, H., Pigareva, M.L., Bautista, V., Barcia, C., Herrero, M.T., 2006. Visceral signals reach visual cortex during slow wave sleep: study in monkeys. Acta Neurobiol. Exp. 66 (1), 69–73.

Pigarev, I.N., 1994. Neurons of visual cortex respond to visceral stimulation during slow wave sleep. Neuroscience 62 (4), 1237–1243. doi:10.1016/0306-4522(94)90355-7.

Power, J.D., Mitra, A., Laumann, T.O., Snyder, A.Z., Schlaggar, B.L., Petersen, S.E., 2014. Methods to detect, characterize, and remove motion artifact in resting state fMRI. NeuroImage 84, 320–341. doi:10.1016/j.neuroimage.2013.08.048.

Proctor, C., Thiennimitr, P., Chattipakorn, N., Chattipakorn, S.C., 2017. Diet, gut microbiota and cognition. Metabolic Brain Disease. Springer US doi:10.1007/s11011-016-9917-8.

Rebollo, I., Devauchelle, A.-D., Béranger, B., Tallon-Baudry, C., 2018. Stomach-brain synchrony reveals a novel, delayed-connectivity resting-state network in humans. ELife 7, e33321. doi:10.7554/eLife.33321.

Richter, C.G., Babo-Rebelo, M., Schwartz, D., Tallon-Baudry, C., 2017. Phase-amplitude coupling at the organism level: the amplitude of spontaneous alpha rhythm fluctuations varies with the phase of the infra-slow gastric basal rhythm. NeuroImage 146, 951–958. doi:10.1016/j.neuroimage.2016.08.043.

Rokem, A., Trumpis, M., Perez, F., 2009. Nitime: time-series analysis for neuroimaging data. In: Proceedings of the 8th Python in Science Conference, pp. 68–75.

Rubinov, M., Sporns, O., 2010. Complex network measures of brain connectivity: uses and interpretations. NeuroImage 52 (3), 1059–1069. doi:10.1016/j.neuroimage.2009.10.003.

Salthouse, T.A., 2005. Relations between cognitive abilities and measures of executive functioning. Neuropsychology 19 (4), 532–545. doi:10.1037/0894-4105.19.4.532.

Sanders, K.M., Koh, S.D., Ward, S.M., 2006. Interstitial cells of Cajal as pacemakers in the gastrointestinal tract. Annu. Rev. Physiol. 68 (1), 307–343. doi:10.1146/annurev.physiol.68.040504.094718.

Sarna, S.K., 1985. Cyclic motor activity; migrating motor complex: 1985. Gastroenterology 89 (4), 894–913. doi:10.1016/0016-5085(85)90589-X.

Sewaybricker, L.E., Melhorn, S.J., Askren, M.K., Webb, M.F., Tyagi, V., De Leon, M.R.B., …, Schur, E.A., 2019. Salience network connectivity is reduced by a meal and influenced by genetic background and hypothalamic gliosis. Int. J. Obes. 1–11. doi:10.1038/s41366-019-0361-9.

Shai, I., Schwarzfuchs, D., Henkin, Y., Shahar, D.R., Witkow, S., Greenberg, I., …, Stampfer, M.J., 2008. Weight loss with a low-carbohydrate, mediterranean, or low-fat diet. N. Engl. J. Med. 359 (3), 229–241. doi:10.1056/NEJMoa0708681.

Shen, X., Finn, E.S., Scheinost, D., Rosenberg, M.D., Chun, M.M., Papademetris, X., Constable, R.T., 2017. Using connectome-based predictive modeling to predict individual behavior from brain connectivity. Nat. Protoc. 12 (3), 506–518. doi:10.1038/nprot.2016.178.

Spoormaker, V.I., Schröter, M.S., Gleiser, P.M., Andrade, K.C., Dresler, M., Wehrle, R., …, Czisch, M., 2010. Development of a large-scale functional brain network during human non-rapid eye movement sleep. J. Neurosci. 30 (34), 11379–11387. doi:10.1523/JNEUROSCI.2015-10.2010.

Sporns, O., Tononi, G., Kötter, R., 2005. The human connectome: a structural description of the human brain. PLoS Comput. Biol. 1 (4), 0245–0251. doi:10.1371/journal.pcbi.0010042.

Steinert, R.E., Meyer-Gerspach, A.C., Beglinger, C., 2012. The role of the stomach in the control of appetite and the secretion of satiation peptides. AJP: Endocrinol. Metab. 302 (6), E666–E673. doi:10.1152/ajpendo.00457.2011.

Stice, E., Burger, K., 2019. Neural vulnerability factors for obesity. Clin. Psychol. Rev. 68, 38–53. doi:10.1016/J.CPR.2018.12.002.

Stice, E., Yokum, S., 2016. Neural vulnerability factors that increase risk for future weight gain. Psychol. Bull. 142 (5), 447–471. doi:10.1037/bul0000044.

Stice, E., Yokum, S., 2018. Relation of neural response to palatable food tastes and images to future weight gain: Using bootstrap sampling to examine replicability of neuroimaging findings. NeuroImage 183, 522–531. doi:10.1016/j.neuroimage.2018.08.035.

Tack, J., Deloose, E., Ang, D., Scarpellini, E., Vanuytsel, T., Van Oudenhove, L., Depoortere, I., 2016. Motilin-induced gastric contractions signal hunger in man. Gut 65 (2), 214–224. doi:10.1136/gutjnl-2014-308472.

Tagliazucchi, E., Laufs, H., 2014. Decoding wakefulness levels from typical fMRI resting-state data reveals reliable drifts between wakefulness and sleep. Neuron 82 (3), 695–708. doi:10.1016/J.NEURON.2014.03.020.

Thomson, D.J., 1982. Spectrum estimation and harmonic analysis. Proc. IEEE 70 (9), 1055–1096. doi:10.1109/PROC.1982.12433.

Tomasi, D., Wang, G.J., Wang, R., Backus, W., Geliebter, A., Telang, F., …, Volkow, N.D., 2009. Association of body mass and brain activation during gastric distention: Implications for obesity. PLoS One 4 (8), e6847. doi:10.1371/journal.pone.0006847.

Van Dijk, K.R.A., Sabuncu, M.R., Buckner, R.L., 2012. The influence of head motion on intrinsic functional connectivity MRI. NeuroImage 59 (1), 431–438. doi:10.1016/J.NEUROIMAGE.2011.07.044.

Van Oudenhove, L., Vandenberghe, J., Dupont, P., Geeraerts, B., Vos, R., Bormans, G., …, Tack, J., 2009. Cortical deactivations during gastric fundus distension in health: Visceral pain-specific response or attenuation of “default mode” brain function? A H215O-PET study. Neurogastroenterol. Motil. 21 (3), 259–271. doi:10.1111/j.1365-2982.2008.01196.x.

Verhaeghen, P., 2011. Aging and executive control: reports of a demise greatly exaggerated. Curr. Direct. Psychol. Sci. 20 (3), 174–180. doi:10.1177/0963721411408772.

Wang, G.J., Tomasi, D., Backus, W., Wang, R., Telang, F., Geliebter, A., …, Volkow, N.D., 2008. Gastric distention activates satiety circuitry in the human brain. NeuroImage 39 (4), 1824–1831. doi:10.1016/j.neuroimage.2007.11.008.

Wang, Y., Beydoun, M.A., Liang, L., Caballero, B., Kumanyika, S.K., 2008. Will all americans become overweight or obese? Estimating the progression and cost of the US obesity epidemic. Obesity 16 (10), 2323–2330. doi:10.1038/oby.2008.351.

Wasylyshyn, C., Verhaeghen, P., Sliwinski, M.J., 2011. Aging and task switching: a meta-analysis. Psychol. Aging 26 (1), 15–20. doi:10.1037/a0020912.

Weygandt, M., Mai, K., Dommes, E., Leupelt, V., Hackmack, K., Kahnt, T., …, Haynes, J.D., 2013. The role of neural impulse control mechanisms for dietary success in obesity. NeuroImage 83, 669–678. doi:10.1016/j.neuroimage.2013.07.028.

Yaskolka Meir, A., Tsaban, G., Zelicha, H., Rinott, E., Kaplan, A., Youngster, I., …, Shai, I., 2019. A green-Mediterranean diet, supplemented with Mankai Duckweed, preserves iron-homeostasis in humans and is efficient in reversal of anemia in rats. J. Nutr. 149 (6), 1004–1011. doi:10.1093/jn/nxy321.

Yeo, B.T.T., Krienen, F.M., Sepulcre, J., Sabuncu, M.R., Lashkari, D., Hollinshead, M., …, Roland, P., 2011. The organization of the human cerebral cortex estimated by intrinsic functional connectivity. J. Neurophysiol. 106 (3), 1125–1165. doi:10.1152/jn.00338.2011.

Zalesky, A., Fornito, A., Bullmore, E.T., 2010. Network-based statistic: Identifying differences in brain networks. NeuroImage 53 (4), 1197–1207. doi:10.1016/j.neuroimage.2010.06.041.